

Glassy behavior in a binary atomic mixture

Bryce Gadway,^{*} Daniel Pertot,[†] Jeremy Reeves, Matthias Vogt, and Dominik Schneble
Department of Physics and Astronomy, Stony Brook University, Stony Brook, NY 11794-3800, USA
 (Dated: September 7, 2021)

We experimentally study one-dimensional, lattice-modulated Bose gases in the presence of an uncorrelated disorder potential formed by localized impurity atoms, and compare to the case of correlated quasi-disorder formed by an incommensurate lattice. While the effects of the two disorder realizations are comparable deeply in the strongly interacting regime, both showing signatures of Bose glass formation, we find a dramatic difference near the superfluid-to-insulator transition. In this transition region, we observe that random, uncorrelated disorder leads to a shift of the critical lattice depth for the breakdown of transport as opposed to the case of correlated quasi-disorder, where no such shift is seen. Our findings, which are consistent with recent predictions for interacting bosons in one dimension, illustrate the important role of correlations in disordered atomic systems.

PACS numbers: 67.85.Hj ; 67.85.Fg ; 61.43.-j ; 03.75.Kk

The presence of disorder is inherent to solid state systems, and it has profound effects on transport in a variety of contexts, ranging from electron conductivity in metals to dirty superconductors [1]. Quantum gases in optical lattices [2] can, with a high degree of experimental control, elucidate the role played by disorder in a number of physical phenomena. Recently, Anderson localization of matter-waves in disordered potentials has been observed for non-interacting gases [3, 4], and additionally, the reemergence of superfluidity due to repulsive interactions [5]. Discerning the (at times) competing roles of disorder and interactions is key to the understanding of Bose-glass behavior [6–8] in strongly interacting disordered systems. Ultracold atomic systems [9, 10] should provide a versatile testbed to aid in this endeavor [11].

Previous studies of ultracold atoms in disordered potential landscapes, generated by optical fields, have generally suffered from strong correlations of the disorder that decay over length scales greater than either the healing length of the superfluid or the lattice spacing. This is true for both speckle potentials [3, 10] that are diffraction-limited to structures on the order of the generating laser field’s wavelength, and quasi-disordered bichromatic lattices [4, 5, 9], which over large distances exhibit perfect correlations that may make them rather unsuitable for the realization of true disorder. To circumvent these limitations, recently it has been proposed [12–15] to use atomic impurities, which can be confined to regions much smaller than a lattice spacing, to act as point-like defects.

The sudden quench of an atomic impurity field acting on mobile particles has been proposed [13, 15] for the study of dynamical, out-of-equilibrium response to disorder. Alternatively, theoretical studies [14, 16] have shown that even a slow “freeze-out” of the tunneling of one species from an initially homogenous mixture can lead to metastable “quantum emulsion” states, typified by local separation between frozen and mobile atoms (for repulsive interactions) and displaying properties sim-

ilar to an equilibrium Bose glass. The study of quantum emulsions may help shed light on the coherence-loss mechanism in a number of experiments involving mass-imbalanced atomic mixtures, both for the boson-boson [17] and boson-fermion [18, 19] cases.

Here, we report on experimental studies of interacting one-dimensional (1D) Bose gases in the presence of disorder. We study the effects of uncorrelated disorder formed by atoms of an auxiliary spin state “frozen” to sites of an incommensurate lattice, and compare to the case of correlated quasi-disorder from an incommensurate bichromatic optical lattice. While both disorder types drive strongly interacting samples into an apparent Bose glass state, a large difference is seen for intermediate interactions, where we find that uncorrelated disorder has a dramatic effect in driving the system towards an insulating state. Our observation of enhanced localization for a more random disorder is consistent with recent theoretical predictions for interacting bosons in 1D [20].

The cartoon in Fig. 1 (a) qualitatively depicts our one-dimensional systems of lattice-trapped bosons with embedded impurities. After creating a homogeneous spin mixture, we slowly freeze the impurity atoms to a deep state-selective lattice of incommensurate spacing. For

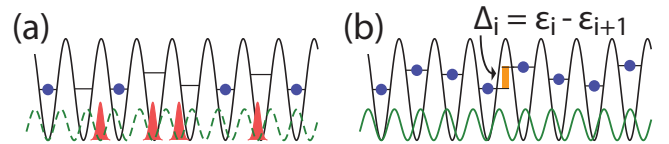


FIG. 1. Disordered one-dimensional Bose gases. (a) To create a disordered impurity-field, half the atoms of a lattice-trapped Bose gas are converted to an auxiliary spin state (red) and localized to a state-selective incommensurate lattice (dashed green). (b) Alternatively, a weak incommensurate lattice (green) is superimposed onto a lattice-trapped Bose gas. In both cases, the secondary potential (atomic or optical) causes site-dependent energy shifts ϵ_i and site-to-site energy differences Δ_i .

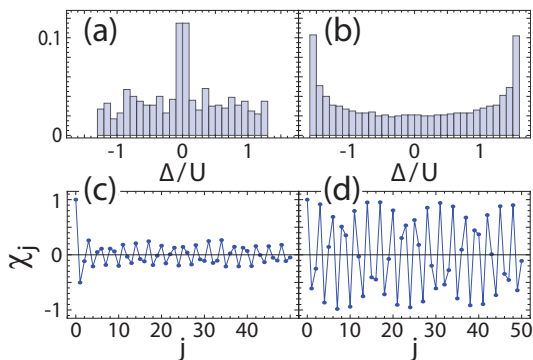


FIG. 2. (a,b) Histograms of calculated Δ -distributions for the cases of the mixture (assuming either 0 or 1 impurities per site) and an incommensurate lattice of depth $s' = 1$. Both are for a primary lattice depth $s = 6$ ($U/E_R = 0.4$). (c,d) The autocorrelation function $\chi_j = \langle \Delta_i \Delta_{i+j} \rangle_i / \langle \Delta_i \Delta_i \rangle_i$ of the Δ -distributions in (a,b), as a function of the site-to-site distance j . The averaging is over 1000 sites.

comparison to a well-studied case of correlated disorder, we also study bosons in an incommensurate bichromatic lattice system [4, 5, 9], as depicted in Fig. 1 (b).

In both cases, the dynamics of the mobile atoms may approximately be described by the Bose–Hubbard Hamiltonian (BHH) [7, 21] $\hat{H} = -t \sum_i (\hat{a}_i^\dagger \hat{a}_{i+1} + \hat{a}_{i+1}^\dagger \hat{a}_i) + \frac{U}{2} \sum_i \hat{n}_i (\hat{n}_i - 1) + \sum_i \hat{n}_i \varepsilon_i$, where t and U are the tunneling and interaction energies of the mobile atoms, and \hat{a}_i , \hat{a}_i^\dagger , and $\hat{n}_i = \hat{a}_i^\dagger \hat{a}_i$ are the annihilation, creation, and number operators for particles at lattice site i . The disordering potentials will generally have two effects - to slightly modify the on-site wavefunctions of the atoms and to cause random site-dependent energy shifts ε_i . The first effect will lead to a spread of site-dependent values for both t and U (with a multi-band treatment necessary for strong perturbations). The second leads to random site-to-site energy differences $\Delta_i = \varepsilon_i - \varepsilon_{i+1}$, which define the resonance conditions for single-particle intersite tunneling. In general, the many-body character will be defined by a competition between energy scales t , U , and Δ , with some dependence on the details of the Δ -distribution [7].

The two disorder potentials of Fig. 1 lead to quite different Δ -distributions. In Fig. 2 we plot calculated histograms for (a) a fifty-percent impurity mixture and for (b) a weak incommensurate lattice (depth $s' = 1$, see experimental description below). While both distributions are continuously filled and extend beyond $\pm \Delta/U$, the details differ considerably. The impurity distribution is peaked about $\Delta/U = 0$ due to adjacent impurity-free sites, while the bichromatic lattice distribution is peaked at the outer-bounds of the distribution. In Fig. 2 (c,d) we plot the normalized autocorrelation function $\chi_j = \langle \Delta_i \Delta_{i+j} \rangle_i / \langle \Delta_i \Delta_i \rangle_i$. The perfectly regular correlations in Fig. 2 (d) are a known attribute of quasi-disordered incommensurate lattices [20, 22]. In contrast, for the

atomic impurity field - combining the irregular spacing of bichromatic lattices and the irregular, probabilistic filling of binary disorder - off-site correlations are strongly suppressed. This difference can have profound effects, as the localization properties of a system will generally depend both the strength and correlation length of the disorder potentials [23]. An extreme case can be found for non-interacting particles in 1D, where random disorder leads to Anderson localization for any finite disorder strength $\Delta \neq 0$, while incommensurate lattices induce localization only beyond a critical lattice depth [4, 24].

To briefly describe our experimental system, we begin as in [25] with an optically trapped Bose–Einstein condensate of ^{87}Rb atoms. In 200 ms we load an array of isolated, one-dimensional tubes formed by the intersection of two optical lattices. These lattices are of period $d = \lambda/2$ and depth $40 E_R$ (with $\lambda = 1064$ nm, $E_R = (h/\lambda)^2/2m$, Planck’s constant h , m the atomic mass). The atoms are trapped along the tube axis z by a nearly harmonic potential of trapping frequency $\omega_z/2\pi = 80$ Hz. A lattice along z , also of period d and with variable depth s (in units of the recoil energy E_R), is smoothly ramped up within 100 ms. This *primary* lattice serves to define the sites (index i) and parameter values (t , U) of the BHH.

Initially, the tubes contain only atoms in the $|F, m_F\rangle \equiv |2, -2\rangle$ hyperfine ground state. To create atomic impurities as in Fig. 1 (a), a fraction (f_{imp}) of the total population of 8×10^4 atoms is transferred to the $|1, -1\rangle$ state via a microwave Landau–Zener sweep. The impurity atoms are loaded into a completely state-selective lattice [25] along z in 20 ms. This lattice has spacing $d' = \lambda'/2$, with $\lambda' = 785$ nm, and the impurity atoms are deeply localized at $20 E'_R$ (recoil energy $E'_R = (h/\lambda')^2/2m \sim 1.8 E_R$).

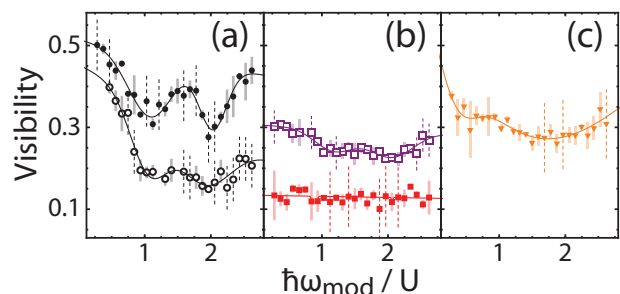


FIG. 3. Disappearance of excitation gap due to disorder. (a) Visibility as a function of amplitude modulation frequency (normalized to $U/E_R = 0.53$ for $s = 14$), in the absence of disorder for $s = 9$ and $s = 14$ (open and filled black circles). Fit lines are two Gaussians on a linear slope. (b) For $s = 14$, with atomic impurities, open purple squares and filled red squares represent $f_{\text{imp}} = 0.1$ and 0.5 , respectively. (c) For $s = 14$, with an incommensurate lattice of depth $s' = 1$ (orange triangles) and no impurities. Solid error bars are statistical over several runs, while dashed are estimated errors for individual runs (120% of maximum statistical error).

We typically study an equal mixture ($f_{\text{imp}} = 0.5$) of frozen and mobile atoms, which we shall refer to as “the mixture”. For the alternate disorder implementation of Fig. 1 (b), we begin with a sample of 4×10^4 atoms in the state $|2, -2\rangle$ (i.e. same number of mobile atoms). We then ramp up a secondary lattice in 20 ms, of spacing d' and variable depth $s' \times E'_R$, onto the $|2, -2\rangle$ atoms. Due to the external trapping potential, our system is not homogeneous, but can be characterized by a typical central filling factor of $\bar{n} \sim 3$ (total) atoms per site.

We begin our investigation into the effects of disorder by measuring excitation spectra, which relate most directly to the distribution of site-to-site energy shifts. Along with a finite compressibility [26], a gapless excitation spectrum is a characteristic feature distinguishing a disordered Bose glass state from a (homogenous) Mott insulator. We measure the excitation spectra by performing amplitude-modulation spectroscopy [9, 27, 29] of the primary z -lattice at driving frequencies $\omega_{\text{mod}}/2\pi$ [30]. For the disorder-free case ($\Delta_i \approx 0$) in Fig. 3 (a), with the sample chosen to be deep into the 1D Mott regime ($s = 14$, $U/t \approx 66$), the excitation spectrum exhibits resonant structure. The resonance positions are consistent with the excitation of particle-hole pairs at U/h [27, 31] (and $2U/h$ due to either higher-order processes or excitation at the edge of Mott domains [27, 31]). In contrast, for both the atomic impurity mixture (Fig. 3 (b)) and for an incommensurate lattice of depth $s' = 1$ (Fig. 3 (c)) having comparable Δ -distribution bounds, we observe flat excitation spectra (cf. [9]). These observations are expected [7] for broadly-filled Δ -distributions with bounds $\Delta_{\text{max}} > U$, and are consistent with the system being in a Bose glass state (future compressibility measurements [26] should allow for the disambiguation between a true Bose glass [7, 8] and a disordered Mott state [28]).

While the observed spectral properties are consistent with Bose glass formation, transport measurements are necessary to confirm insulating behavior. Here, we study the effects of disorder in the transition region between superfluid and insulator, determining the critical lattice depth at which the systems become insulating through the study of localization and transport. In regard to the former, the momentum-peak width of a released sample (related to the inverse correlation length ξ^{-1} of the sample in-situ [32]), exhibits a sudden increase accompanying an abating superfluid fraction and loss of off-diagonal long-range order [33]. As for the latter, it has been shown [27, 34] that the response to an applied impulse dies away upon entering the strongly correlated regime, and can serve as a signature of insulating behavior [10, 29].

To study transport, we look at how the system evolves after an applied impulse. A magnetic-field gradient along z is pulsed on for duration of $T = 1.2$ ms and applies a variable force F ranging from 0 to $F_{\text{max}}/m = 1.2$ m/s², resulting in an impulse $I = F \times T$. As illustrated in

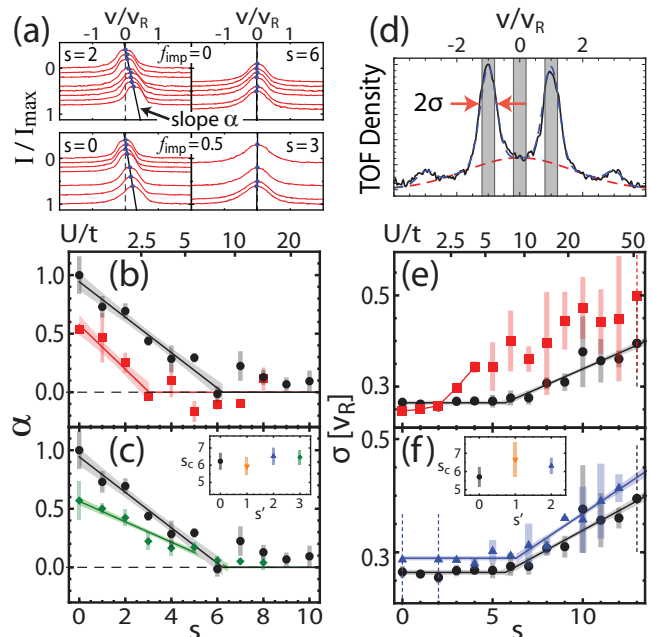


FIG. 4. (a) The response to impulse is determined by a straight-line fit (with slope α , normalized to the case of free atoms) to the dependence of velocity on applied impulse I (profiles shown for disorder-free and impurity mixture cases; recoil velocity $v_R = h/2md$). (b) α versus lattice depth s for bosons without disorder (black circles) and with atomic impurities ($f_{\text{imp}} = 0.5$, red squares). Lines and surrounding shaded regions are fits to the data with confidence regions (1 s.d.) of a linearly decaying response, with no response ($\alpha = 0$) beyond a depth s_c . (c) Similarly, but for an incommensurate lattice ($s' = 3$, green diamonds), with disorder-free data reproduced for comparison. The inset shows values of s_c versus s' as determined by fit intercepts. (d) The momentum-peak width σ ($1/\sqrt{e}$ half-width) is determined by a symmetric multi-Gaussian fit to time-of-flight interference patterns. The shaded regions about $v/v_R = 0(\pm 1)$ are used to count $N_{0(\pm 1)}$ for visibility measurements of Fig. 3. (e) σ versus s for 1D bosons without disorder and for the mixture (colors/symbols as in (b)). The straight line for the disorder-free data is a fit of a linear increase beyond a depth s_c . The first few data points for the case of atomic impurities are connected as a guide to the eye. (f) Similarly, but for an incommensurate lattice with $s' = 2$ (blue triangles) and with disorder-free data reproduced.

Fig. 4 (a), we characterize the response as a function of I (with slope α) by monitoring the center-of-mass velocity along z in time-of-flight absorption images following a brief (~ 1 ms) ramp-off of the z -lattice. We access the momentum-peak width as in [9, 27] by releasing the atoms in time-of-flight following a $50 \mu\text{s}$ lattice ramp up to $s = 20$ and a gravitational phase-shift along z (without impulse or lattice ramp-off). We then determine the peak width σ by a fit to the profile of symmetric diffraction peaks on top of an incoherent background, as shown in Fig. 4 (d).

We find that for the impurity mixture, the mobile

atoms are more easily driven towards insulating behavior. Similar to [29], we determine the critical point at which the atoms become unresponsive to impulse by fitting a linear decay to the response α as a function of lattice depth. As shown in Fig. 4 (b), this fit to the transport measurements yields a critical depth $s_c = 3.0 \pm 0.5$. While we do not fit the peak width data, a kink near $s_c \approx 2$ can be observed in Fig. 4 (e). These values are roughly half of those measured for the disorder-free case, with values of $s_c = 6.2 \pm 0.5$ and 5.7 ± 0.5 based on impulse response and peak width, respectively. This value of $s_c \approx 6$ is close to our expectations based on the mean Lieb–Liniger parameter [35] ($\gamma = 0.6$) of our 1D gases prior to lattice-loading, with an estimate based on the Bose–Hubbard (Sine–Gordon) model predicting $s_c = 6.2$ (4.7) [29].

For the incommensurate lattice, transport data for $s' = 3$ is shown in Fig. 4 (c). In this case no shift of the critical depth is seen, and as shown in the inset, this is the case for all incommensurate lattice depths considered ($s' \leq 3$, where we restrict to $s'/s < 1$ in the transition region to maintain the perturbative nature of the incommensurate lattice). The momentum-peak width data mirrors this lack of a shift of the transition point (inset: for all depths considered $s' \leq 2$).

While both incarnations of disorder resulted in an apparent Bose glass state for very deep lattices, a clear difference was seen in their effect on more weakly interacting samples. In attempting to account for the observed difference, a natural consideration is the disparity in their correlations [χ_j , cf. Fig. 2 (c,d)]. In general, one expects that the less correlated the disorder, the more enhanced is the localization [23]. For interacting bosons in 1D, it has been shown theoretically [20] that the localization transition occurs for a more weakly interacting gas (larger values of the Luttinger exponent K or lower values of the Lieb–Liniger parameter γ [24]) in uncorrelated disorder than for correlated disorder. Our observations of a sizeable shift of the transition point for impurities and a negligible shift for an incommensurate lattice are thus in qualitative agreement with expectations based on their dissimilar correlation properties.

Also relevant to our observations is the reduction of phase-space density in the presence of localized impurities, as well as of the atomic density due to the dynamical formation of impurities from the mobile species. The first effect has been shown [36] to be responsible for adiabatic heating and loss of coherence in recent Bose–Fermi mixture experiments [19], due to reduced entropy following a reduction in effectively occupiable sites, both for attractive and repulsive interactions. The second effect is more particular to “quantum emulsion” [14, 15, 25] experiments. Here, reduced density leads to more strongly correlated many-body states in 1D and thus favors increased localization and insulating behavior.

In conclusion, we have observed signatures of Bose glass formation in 1D Bose gases with superimposed

disorder, both for atomic impurities and for quasi-disordered bichromatic lattices. The two disorder types have dramatically different effects in the transition region between superfluid and insulator, with atomic impurity disorder inducing localization in much more weakly interacting gases. Our observation that a more weakly correlated disorder leads to enhanced localization is in qualitative agreement with recent theoretical predictions for interacting 1D boson systems.

We thank Martin G. Cohen for valuable comments on the manuscript. This work was supported by NSF (PHY-0855643) and the Research Foundation of SUNY. B.G. and J.R. acknowledge support from the GAANN program of the US DoEd.

* bgadway@ic.sunysb.edu

† Present address: AMOP Group, Cavendish Laboratory, University of Cambridge, Cambridge, United Kingdom

- [1] P. W. Anderson, *Journal of Physics and Chemistry of Solids* **11**, 26 (1959).
- [2] I. Bloch, J. Dalibard, and W. Zwerger, *Rev. Mod. Phys.* **80**, 885 (2008).
- [3] J. Billy *et al.*, *Nature* **453**, 891 (2008).
- [4] G. Roati *et al.*, *Nature* **453**, 895 (2008).
- [5] B. Deissler *et al.*, *Nat Phys* **6**, 354 (2010).
- [6] T. Giamarchi and H. J. Schulz, *Phys. Rev. B* **37**, 325 (1988).
- [7] M. P. A. Fisher *et al.*, *Phys. Rev. B* **40**, 546 (1989).
- [8] W. Krauth, N. Trivedi, and D. Ceperley, *Phys. Rev. Lett.* **67**, 2307 (1991).
- [9] L. Fallani *et al.*, *Phys. Rev. Lett.* **98**, 130404 (2007).
- [10] M. White *et al.*, *Phys. Rev. Lett.* **102**, 055301 (2009); M. Pasienski *et al.*, *Nature Physics* **6**, 677 (2010).
- [11] L. Sanchez-Palencia and M. Lewenstein, *Nature Physics* **6**, 87 (2010).
- [12] U. Gavish and Y. Castin, *Phys. Rev. Lett.* **95**, 020401 (2005).
- [13] B. Paredes, F. Verstraete, and J. I. Cirac, *Phys. Rev. Lett.* **95**, 140501 (2005).
- [14] T. Roscilde and J. I. Cirac, *Phys. Rev. Lett.* **98**, 190402 (2007).
- [15] B. Horstmann, S. Dürr, and T. Roscilde, *Phys. Rev. Lett.* **105**, 160402 (2010).
- [16] P. Buonsante *et al.*, *Phys. Rev. Lett.* **100**, 240402 (2008).
- [17] J. Catani *et al.*, *Phys. Rev. A* **77**, 011603 (2008).
- [18] S. Ospelkaus *et al.*, *Phys. Rev. Lett.* **96**, 180403 (2006); K. Günter *et al.*, *ibid.* **96**, 180402 (2006).
- [19] T. Best *et al.*, *Phys. Rev. Lett.* **102**, 030408 (2009).
- [20] G. Roux *et al.*, *Phys. Rev. A* **78**, 023628 (2008).
- [21] D. Jaksch *et al.*, *Phys. Rev. Lett.* **81**, 3108 (1998).
- [22] T. Roscilde, *Phys. Rev. A* **77**, 063605 (2008).
- [23] P. Lugan *et al.*, *Phys. Rev. Lett.* **98**, 170403 (2007); R. C. Kuhn *et al.*, *New J. Phys.* **9**, 161(2007).
- [24] M. A. Cazalilla *et al.*, arXiv:1101.5337(2011); And references therein.
- [25] B. Gadway *et al.*, *Phys. Rev. Lett.* **105**, 045303 (2010).
- [26] D. Delande and J. Zakrzewski, *Phys. Rev. Lett.* **102**, 085301 (2009).

- [27] T. Stöferle *et al.*, Phys. Rev. Lett. **92**, 130403 (2004).
- [28] D. Heidarian and N. Trivedi, Phys. Rev. Lett. **93**, 126401 (2004).
- [29] E. Haller *et al.*, Nature **466**, 597 (2010).
- [30] We sinusoidally modulate s by $\pm 15\%$ for 80 ms, ramp down to $s = 4$ in 5 ms, and allow 15 ms of thermalization. When used, the incommensurate lattice is turned on in 20 ms prior to modulation and off in 5 ms concurrent with primary lattice ramp-down. From time-of-flight interference we measure the visibility η_-/η_+ [25], with $\eta_{\pm} = N_{+1} + N_{-1} \pm 2N_0$; $N_{0(\pm 1)}$ apertures in Fig. 4 (d).
- [31] M. Greiner *et al.*, Nature **415**, 39 (2002).
- [32] C. Kollath *et al.*, Phys. Rev. A **69**, 031601 (2004).
- [33] S. Trotzky *et al.*, Nature Physics **6**, 998 (2010).
- [34] C. D. Fertig *et al.*, Phys. Rev. Lett. **94**, 120403 (2005).
- [35] $\gamma = mg_{1D}/\hbar^2 n_{1D}$ [24], with effective 1D interaction strength $g_{1D} \approx 2\hbar\omega_{\perp}a$ [37], s-wave scattering length $a \approx 5.3$ nm, and transverse trapping frequency $\omega_{\perp} = 2\pi \times 26$ kHz. For the 1D density n_{1D} , we assume a Thomas–Fermi profile and take a weighted tube-average of $2/3 \times$ the density at the center of each tube.
- [36] M. Snoek *et al.*, Phys. Rev. Lett. **106**, 155301 (2011); M. Cramer, Phys. Rev. Lett. **106**, 215302 (2011).
- [37] M. Olshanii, Phys. Rev. Lett. **81**, 938 (1998).